Fabrication of Quantum Optical Elements with InN Nanoparticles for Quantum Dots Solar Concentrator

Jun Togami*, Hiroshi Takano and Masayuki Itoh[1]

[1] Department of Chemical Engineering and Materials Science, Doshisha University,

Kyotanabe, Kyoto 610-03, Japan

* Jun Togami, mito@mail.doshisha.ac.jp

Abstract

To enhance the efficiency of luminescent solar concentrators with PV cells made of p-n junction, an optical element made of InN nanoparticle thin layer was fabricated with the quantum dot physical deposition process. The geometric mean diameter and standard deviation of the InN particles were 4.6nm and 1.33, respectively. The particle number density at the surface of the QDSC element was 1.01×10^{12} particles/cm^2. The particle number density was very high comparing with any other studies, however, it was still not high enough to use for our QDSC. The photoluminescence of thin borosilicate glasses fitted the desirable theoretical wavelength of our QDSC absorption spectrum. The longer wavelength the excitation spectrum shifted, the shorter the emission spectrum due to the effect of the InN QDs shifted. The excited PL intensity difference was so larger. Although the completion of our QDSC remained a distant goal, it was found that the conversion efficiency with our QDSC increased 8.5% compared with only one cell. It was thought that the QDSC down-converted wavelength of near-UV radiation not ever being available in solar spectrum became available for the a-Si PV cell.

Keywords: luminescent solar concentrator, frequency shifter, InN quantum dots, QDPD method

1. Introduction

A solar concentration technique to use full spectrum of solar radiation efficiently becomes important because the density of solar energy is mostly 1kW/m^2 in Japan [1]. A concentrator is usually defined as a geometric optical light equipment to collect and condense solar light over a large area to illuminate onto a smaller area like a solar cell. In contrast, the third generation of solar cells such as a luminescent solar concentrator is broadly defined as a semiconductor device which does not rely on a traditional p-n junction to separate photogenerated charge carriers. The luminescent concentrator shows several potential advantages. One is that both for direct and diffuse radiation can be collected easily. Another advantage is the cost reduction of photovoltaic power generation by concentration of light [2]. It is thought that the development of solar cells in the third generation will act a major role in the innovation of the material, which includes new utilization of existing materials and principles. These new devices are so called quantum dots solar concentrator (QDSC) [3]. The degree of red shift between absorption and luminescence of incident light via quantum dots (QDs) is determined by the bandgap of QDs, and the bandgap is controllable by changing the diameter. Full spectrum utilization of solar energy helps the energy conversion efficiency to be more than 60% [4]. Such high theoretical limit on the conversion efficiency by the QDSC means substantial improvements of current commercial solar cells, both silicon and thin-film based. In this study, the method and some results were described especially on the fabrication of the quantum optical elements as frequency shifter for the QDSC with quantum dot physical deposition (QDPD) method [5] for production of InN QDs.

2. Motivation and theory

2.1. The construction of QDSC

QDs are semiconducting crystals of nanometer size with a tunable bandgap of energy levels that react as a special class of semiconductors composed of periodic groups of II-VI, III-V, or IV-VI materials. The use of QDs can turn the old concept of a luminescent solar collector into a practical concentrator. If QDs with high quantum efficiency (QE) can be built into a transparent media, the QDSC that performs in the upper range of efficiency predicted for dye concentrators may be realized [6]. Energy whose wavelength is shorter than bandgap wavelength of Si transmits without absorption, which comes to the loss around 15-19% toward total energy in sunlight, because solar spectrum consists of wide wavelength. Meanwhile, if sunlight whose energy is larger than bandgap energy falls on the surface of the QDSC, high-energy electron is subjected to excitation. The electron reaches the conduction band and hole reaches the valence band. Then the energy is lost between several tens of femtosecond and several picoseconds, and it eases to each band-edge. This energy loss of short wavelength side becomes about 30%, which causes the limit to the conversion efficiency of conventional solar cells. These lost energy comes to heat, this heat also causes the depression of the solar cells efficiency. Therefore, solar concentrators can reduce the cost of solar power since more electricity is obtained per solar cell, and fewer solar cells are needed. Moreover, the QDSC is perfectly different energy enhancer based on the quantum size effect of nanoparticles [3]. The structural concept of our QDSC was shown in Fig. 1. Quantum optical element was constructed with stacked thin borosilicate glass plates (3.0cm×4.5cm×0.14cm) covered by InN QDs. Photons were isotropically reemitted with the down-converted frequency dependent on QD size. A large proportion of the emitted photons would be trapped within the plate and transported to the edges by total internal reflection. Reflective mirrors were mounted on the three edges and on the back surface, so light could only reach to the fourth edge where it was absorbed by a photovoltaic cell [7].

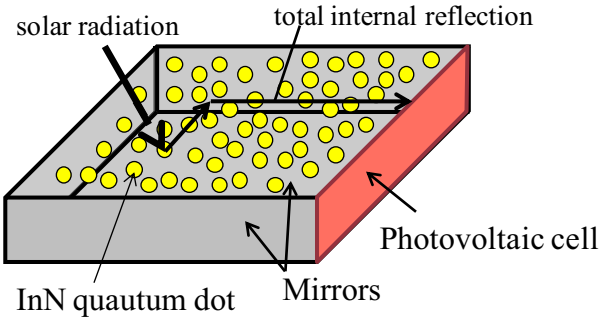

Fig. 1. A structural concept of our QDSC.

2.2. Down-conversion frequency shifter with InN QDs

InN has extremely-attractive property as an ultrafast electron device because the effective mass of electron is lower than other semiconductors, and electron-hole transfer rate is high under highly field intensity [8]. The bandgap of the QDSC is varied according to the diameter of InN QDs. Fig. 2 indicates the dependence of the bandgap on QD diameter. As shown in Fig. 2, the bandgap increased when the size of the QDs became smaller. The quantum effect is apparent in smaller QDs, because the effect occurs around the size of the Bohr diameter. In this trial for QDSC

construction, the diameters of InN QDs were set to 5, 6 and 13 nm connecting to the emit lights of blue, green and red colors, respectively [9].

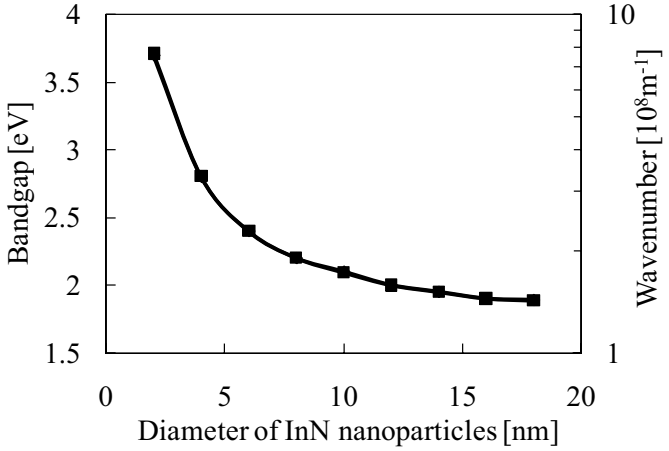

Fig. 2. Bandgap of InN nanoparticles in each their diameter.

2.3. Theoretical conversion efficiency of the QDSC

The photons absorbed by QDs are reemitted having lower frequency due to down-conversion, and eventually photoelectric converted by reaching PV cells. The higher QD concentration signifies much availability of solar energy, still the probability of photon re-absorption by other QDs also becomes high in such particle concentration. Estimation on the optimal particle concentration is very important concerning the relationship between particle concentration and theoretical conversion efficiency of the QDSC. The efficiency is analytically calculated with the types of PV cells and QDs, leaked energy to outside of the QDSC, and re-absorption by QDs. As the first step, ζ the ratio of the energy available to absorb QDs is calculated on the bandgap of PV cells. If Si is used for the cell, ζ is 0.64 [10]. The efficiency of the QDSC, η_{qdsc}, is calculated with the following equation.

$$\eta_{\mathrm{qdsc}} = \eta_{\mathrm{pvc}}\left[\eta(1-P)\right]^{1+r} S/I\,\xi \tag{1}$$

where η the quantum efficiency of QDs, P the probability of photons leaked by total inner reflection, r the re-absorption ratio, S the flux of solar energy reaching the PV cell, I the total solar energy, η_{pvc} the conversion efficiency of only the cell. With n the refractive index of a glass, P is definded as

$$P = 1-\left(1+1/2n^2\right)\left(1-1/n^2\right)^{1/2} \tag{2}$$

r is given by

$$r = \int_0^{\infty} f(\nu)\left\{1-\exp\left[-\alpha(\nu)l\right]\right\}d\nu \tag{3}$$

where l the path length over which re-absorption can occur, $f(\nu)$ the normalized luminescence spectrum, and $\alpha(\nu)$ the absorption coefficient. With A the top area of the glasses, the constant c_s (0.534, in case that cuboid) [11], the molar concentration C, and the absorbance index $\varepsilon(\nu)$, l and $\alpha(\nu)$ are expressed as

$$l = c_s \sqrt{A} \tag{4}$$

$$\alpha(\nu) = C\varepsilon(\nu)\ln(10) \tag{5}$$

I and *S* are defined as follow equation.

$$I = \int_0^{\infty} d\nu \int_0^{\pi/2} d\theta_i N(\nu) U(\theta_i, \nu) \sin(\theta_i) \cos(\theta_i) \tag{6}$$

$$S = \int_0^{\infty} d\nu \int_0^{\pi/2} d\theta_i T(\theta_i, \nu) N(\nu) U(\theta_i, \nu) \frac{\alpha(\nu)}{\alpha_t(\nu)} \times \{1 - \exp[-\alpha_t(\nu) l]\} \sin(\theta_i) \cos(\theta_i) \tag{7}$$

where θ_i the incident angle to the surface of a top glass, $N(\nu)$ the incident solar flux, $T(\theta_i,\nu)$ times the transmission coefficient for entering the QDSC, $\alpha(\nu)/\alpha_t(\nu)$ times the fraction which specifies how much the absorbed flux was absorbed by the QDs, $U(\theta_i,\nu)$ the normalized solar spectrum. As above, the theoretical efficiency of the QDSC resulted in 9.79% when high densely QDs (QE > 0.9) is necessary such as InN QDs using in the glasses. Therefore, it is thought that the QDSC can be created, to be lower in cost and higher in efficiency than existing one.

3. Experimental method

The QDs were fabricated with QDPD method as followings; Fig. 3 shows the schematic diagram of QDPD aparatus. InN powder was filled in an Al_2O_3 crucible set in an evaporation chamber. Pressure in the chamber was stabilized with a mechanical booster pump (Mitsubishi Electric SF-ERF), two rotary pumps (ULVAC D-330K) and a diffusion pump (ULVAC ULK-06A). The crucible temperature was set at 576K, and QDs nucleated with the vaporized In-N_2 gases were carried to the deposition part following the growth part of the chamber along to the carrier gas flow of He (99.995%). He gas went through the drying and deoxidizing column, and the total inner gas pressure of InN and He was changed from 170 to 6.9Pa.The InN QDs were deposited onto glass plates and carbon micro-grids with the thermophoretic cold trap system. Growth time of QDs was changed 60-180s, and the produced InN QDs were observed and characterized with transmission electron microscope (TEM).

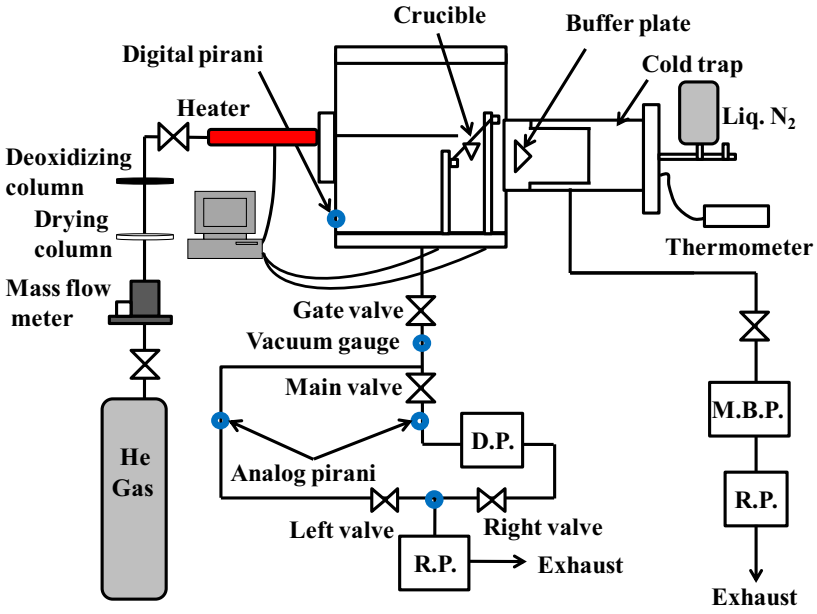

Fig. 3. A schematic diagram of QDPD apparatus.

The photoluminescence from samples were measured with spectrophotofluorometer (JASCO FP-6500). The value of current and voltage were measured with the circuit tester (HIOKI Model 3002) when solar light was directly irradiated to the samples.

4. Results and discussion

4.1. Optimization of the InN QDs size

TEM images of InN nanoparticles on the carbon micro-grid were shown in Fig. 4. In Fig. 4(a), the geometric mean diameters d_g and standard deviation σ_g of the particles generated at 170Pa were 44.5 nm and 1.58, respectively. The existing highly dispersed but crystallized large particles indicated that the particles were not original ones but the islands produced on the substrate by the mutual fusion of liquefied QDs deposited nearby one other [12]. Such islands often appear after the deposition of particle cloud called puff under the condition of slightly higher vapor pressure of specimen and carrier gas. To avoid such mutual fusion of deposited particles, the QDSC element was fabricated at lower total pressure of 37Pa. As shown in Fig. 4(b), d_g and σ_g of the case was 5.7nm and 1.17 and the particle number density was 2.13×10^{10} particles/cm^2. Although the particle size was more suitable, the particle density was still not enough to use as a quantum optical element of our QDSC. High particle density requires high particle concentration via nucleation. In particulate process, coagulational growth is dominant in high concentration rather than condensational growth. In such case, it is essential point how to set shorter time for particle transport from nucleation point to the substrate position. The ideal condition is that the particle should nucleate nearby the substrate. To refer on the detail of such particle generation technique is beyond the field of this report, but it is possible to use a large buffer plate just after the growth part of chamber to remove the particle nucleated at the growth part. For this reason, the buffer plate was improved and the experimental condition was changed; total inner pressure and the growth time was set to 6.9Pa and 180s. Under this condition, TEM image of InN nanoparticles was shown in Fig. 4(c), d_g and σ_g of the case was 4.6nm and 1.33 and the particle density was 1.01×10^{12} particles/cm^2. The quantum optical element with these values is suitable for our QDSC.

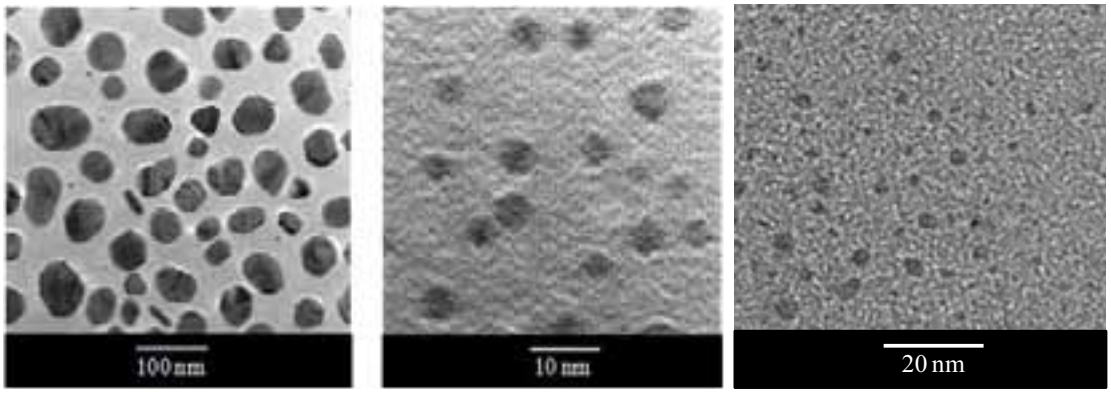

(a) (b) (c)

Fig. 4. TEM images of InN nanoparticles on the carbon micro-grid, total inner pressure: (a)170Pa, (b)37Pa, (c)6.9Pa and with the large buffer plate.

4.2. Photoluminescent measurement

By changing the excitation spectrum of irradiation light to 220, 240, 260, 280, 300nm, the photoluminescence with the borosilicate glass 0.14mm thick was measured, respectively. Fig. 5 shows the results of the emission spectra. The emission intensity rises according to the shifting of

excitation spectrum toward shorter wavelengths. It was thought that the original intensity of irradiation light was stronger as this reason. In addition, the emission spectrum shifted toward shorter wavelengths. From this result, it was found that the limited excitation wavelength of the glass was around 350nm. This is why the results are matched to the desirable theoretical wavelength of our QDSC absorption spectrum.

The photoluminescence was measured on the three types of samples, only a borosilicate glass, the glass deposited the thinned InN, and the glass deposited the InN QDs. The emission photoluminescence (PL) from the glass attached the InN QDs was stronger than the other two samples. This shift towards higher intensity might be caused by quantum effect of InN nanoparticles. Fig. 6 shows the PL difference by changing the excitation spectrum of irradiation light to 280, 300nm. Here, the longer wavelength the excitation spectrum shifted, the shorter the emission spectrum due to the effect of the InN QDs shifted, and the PL difference was so larger. The result also showed that the glass with deposited InN QDs on the QDSC is effective for the improvement of the conversion efficiency.

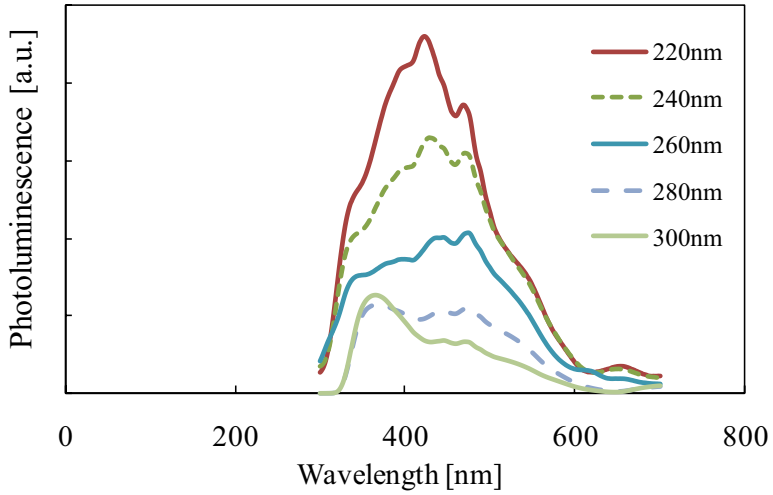

Fig. 5. Emission spectra for the thin borosilicate glass.

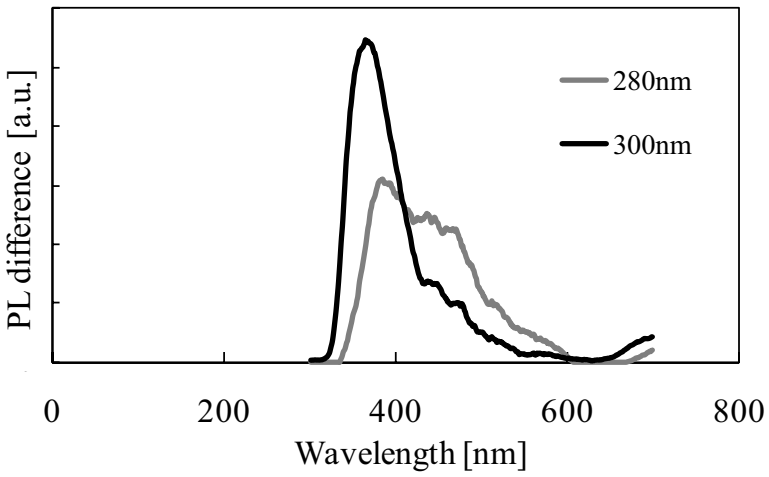

Fig. 6. PL difference between only a glass and the glass with InN QDs.

4.3. Energy conversion efficiency of QDSC

Table 1, 2 show the results of the short-circuit current, open-circuit voltage and conversion efficiency when solar light was irradiated on the amorphous Si (a-Si) PV cell (3.0cm×1.0cm). Only one s-Si PV cell was applied on the side edge of the glasses in the case of Table 1. In Table 2, the cells were set on the both side of the glass edge and these two solar cells were connected in series. The efficiency using the glass was lower than the cell without the glass as shown in Table 1. However, as shown in Table 2, the application of stacked glasses as quantum optical elements helps the increase of efficiency because the efficiency with the light of total internal reflection in the stacked seventy glasses was higher than that with a glass. Although the completion of our QDSC remained a distant goal, it was found that increment of the conversion efficiency, 8.5%, was accomplished with our QDSC compared with the case of only one cell. Therefore, down-converted wavelength of near-UV radiation shall be available for the a-Si cell using the glass deposited InN QDs. As an alternative, setting PV cells on full perimeter and using a high efficiency CPV cell will more improve our QDSC.

Table 1. Values for each sample's result

Material	I_{SC} [mA]	V_{OC} [V]	η [%]
a-Si PV cell	7.5	3.1	7.8
a-Si PV cell + a glass	3.0	2.8	2.8
a-Si PV cell + seventy stacked glasses	6.8	2.8	6.3
a-Si PV cell + seventy stacked glasses + backside mirror	7.0	2.9	6.8

Table 2. The results in using PV cells on two edges of the glasses

Material	I_{SC} [mA]	V_{OC} [V]	η [%]
Two a-Si PV cells	7.5	6.0	7.5
Two a-Si PV cells (set on short side) + seventy stacked glasses + backside mirror	7.9	6.3	8.3
Two a-Si PV cells (set on long side) + seventy stacked glasses + backside mirror	8.0	6.4	8.5

5. Conclusion

The quantum optical element for the QDSC was fabricated with QDPD method, and it could be available as frequency shifter. The experimental condition should be modified to extend the utilized spectrum, but the produced ODs showed good performance as for the first trial manufacturing of the QDSC. The measured emission spectra for the thin borosilicate glass and PL difference showed the usability of the glasses containing deposited InN QDs. The QDSC down-converted wavelength of near-UV radiation, which was not ever used in solar spectrum, became available for the a-Si PV cell. Furthermore, fabrication of more suitable quantum optical elements with solar concentrator for our QDSC shall be tried to attain high conversion efficiency.

References

[1] M.J. Currie, et al., Science, 321, (2009) 226-228.

[2] L.R. Wilson, et al., Appl. Opt., 49(9), (2010) 1651-1661.

[3] A.J. Nozik, Physica E, 14, (2002) 115-120.
[4] Y. Okada, R. Oshima and A. Takata, J. Appl. Phys., 106, (2009) 024306.
[5] K. Sakiyama, M. Itoh, S. Handoh, and H. Takano, J. Aerosol Sci., 30, (1999) S465-S466.
[6] G. Wilfried, er al., Optics Express, 16, (2008) 21773-21792.
[7] S.J. Gallagher, B. Norton and P.C. Eames, Solar Energy, 81, (2007) 813-821.
[8] A.G. Bhuyan, A. Hashimoto and A. Yamamoto, J. Appl. Phys., 94, (2003) 2779.
[9] T. Morioka, Patent Application Publication, (2005) 0012076 A1.
[10] J.S. Batchelder, et al., Appl. Opt., 18(18), (1979) 3090-3110.
[11] R. Soti, et al., J. Luminescence, 68, (1996) 105-114.
[12] D.V. Talapin, et al., Chem. Rev., 110(1), (2010) 389-458.